RGNZ/MGPB

Susceptibility Assessment of Earthquake-induced Landslides: the 2018 Palu, Sulawesi Mw 7.5 Earthquake, Indonesia

Yukni Arifianti[1]; Pamela[2]; Prahara Iqbal[3]; Sumaryono[4]; Amalfi Omang[5]; Hilda Lestiana[6]

[1] Jl. Sangkuriang, Dago, Kecamatan Coblong (Research Center for Geological Disaster, National Research and Innovation Agency (BRIN), 40135), ORCID 0000-0003-3838-2529

[2] Jl. Diponegoro No.57, Cihaur Geulis, Kec. Cibeunying Kaler (Geological Agency of Indonesia (BGL), Bandung, Indonesia, 40122), ORCID 0000-0002-9598-2187

[3] Jl. Sangkuriang, Dago, Kecamatan Coblong (Research Center for Geological Resources, National Research and Innovation Agency (BRIN), 40135), ORCID 0000-0002-6224-396X

[4] Jl. Diponegoro No.57, Cihaur Geulis, Kec. Cibeunying Kaler (Geological Agency of Indonesia (BGL), Bandung, Indonesia, 40122), ORCID maryono93@gmail.com

[5] Jl. Diponegoro No.57, Cihaur Geulis, Kec. Cibeunying Kaler (Geological Agency of Indonesia (BGL), Bandung, Indonesia, 40122), ORCID amalfi.omang@esdm.go.id

[6] Jl. Sangkuriang, Dago, Kecamatan Coblong (Research Center for Geological Resources, National Research and Innovation Agency (BRIN), 40135), ORCID 0000-0002-2039-5439

Abstract

A catastrophic Palu earthquake on September 28th, 2018 with Mw 7.5 triggered countless slope failures, generating numerous landslides. This paper presents a practical method for susceptibility assessment of earthquake-induced landslides in the Palu region and the surrounding area. The statistical weight of evidence (WoE) model was used to assess the relationship between landslides induced by seismic motion and its causative factors to determine the susceptibility level and derive an earthquake-induced landslide susceptibility map of this study area. The 1273 landslides were classified into two data series, training data for modelling (70%) and test data for validation (30%). The six selected thematic maps as landslide causative factors are lithology, land use, peak ground acceleration (PGA), and slope (gradient, aspect, elevation). The selection of causative factors considerably influences the frequency of landslides in the area. The result is satisfactory because the AUC value of the chosen model excelled the minimum limit, which is 0.6 (60%). The estimated success rate of the model is 85.7%, which shows that the relevancy of the model is good with the occurrence of landslides. The prediction rate of 84.6% indicates that the applied model is very good at predicting new landslides.

Keywords:
earthquake-induced landslide; susceptibility map; Palu earthquake; weight of evidence

1. Introduction

Palu and its vicinity area in Indonesia were struck by a moment magnitude (Mw) of 7.5 earthquakes on September 28th, 2018, at 06:02:44 pm local time (10:02:45 UTC). The main shock and aftershocks severely damaged the area, including other disasters that followed, such as soil liquefaction in plain areas and tsunamis in coastal regions. The National Disaster Mitigation Agency/BNPB reported the newest records on February 5th, 2019, 4,340 fatalities (dead/missing), 4,438 injured, and 172,635 people were displaced due to this disaster (**BNPB, 2019**). The destruction was also followed by countless slope failures in hilly and mountainous areas, generating numerous landslides, which will be the main subject to be discussed later in this paper.

The city of Palu and the surrounding regencies, Sigi and Donggala, are located along the valley of the Palu Koro Fault (PKF) (see **Figure 1A**). This active fault is elongated on the southeast of Palu and continues northwest towards Palu Bay (**Pakpahan et al., 2015**). The USGS reported that the 2018 Palu earthquake resulted from the strike-slip faulting of the PKF (**USGS, 2018**). Previously, the activity of this fault resulted in a series of destructive earthquakes in 1927, 1938, 1968, 1985, 1993, 1996, and 2005 (**Gomez et al., 2000; Bellier et al., 2001; Marjiyono et al., 2013**). Thus, this suggests that Palu is prone to earthquakes and subsequent disasters. Landslides, one of the earthquake's collateral disasters, are posing as the most pervasive in Palu.

The Palu area subjected to the landslide mainly was a highland zone with steep slopes, blocking many road networks, disrupting transportation routes, isolating residential areas, destroying natural resources and artificial

---

Corresponding author: Yukni Arifianti

e-mail address: yukni.a@gmail.com
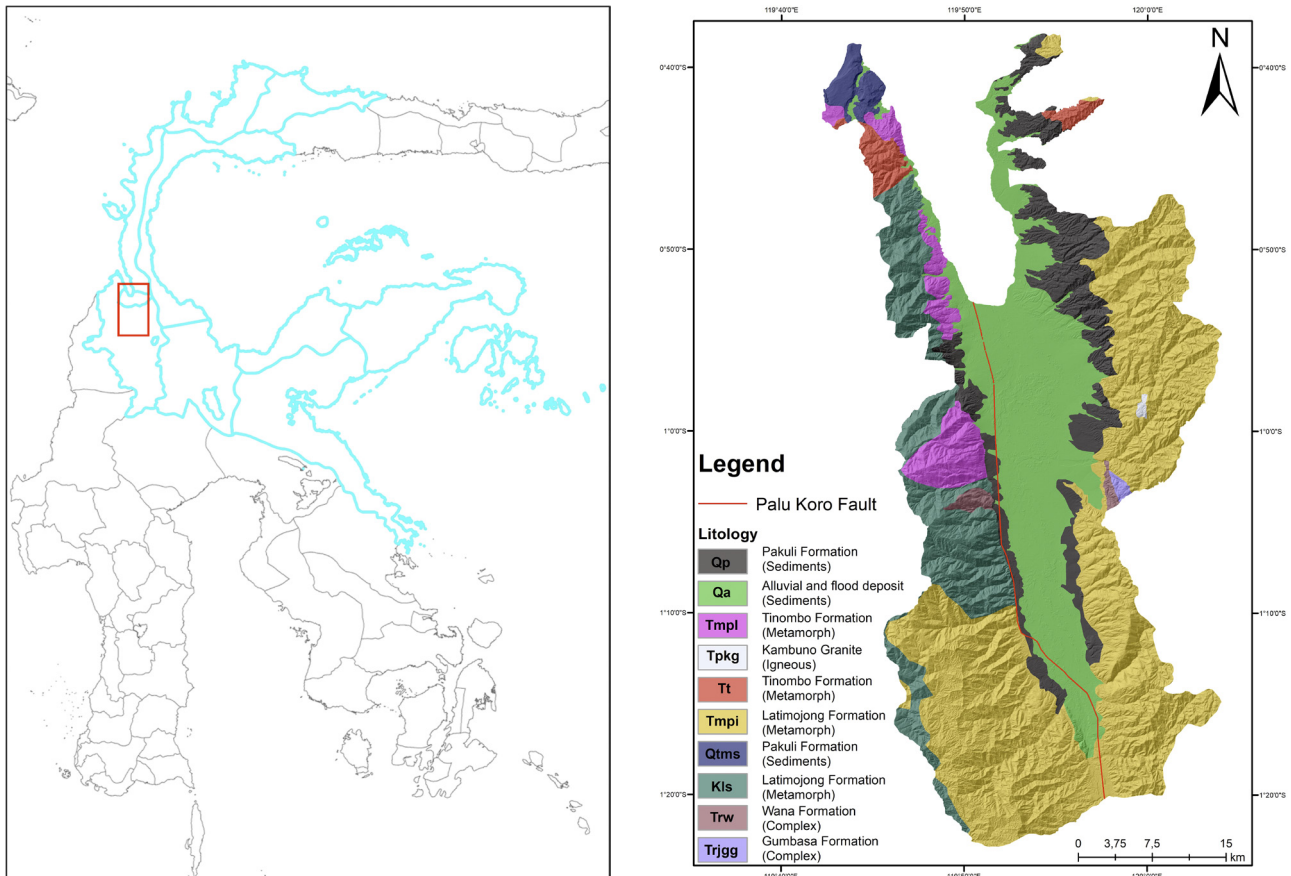
Figure 1: (A) Palu region and the surrounding area, Indonesia (red box); **(B)** Lithology map of the area (modified from **Sukamto (1973)** and **Sukido et al. (1993)**)

infrastructure, and social-economic loss. This fact leads to the importance of the earthquake-induced landslide study. It involves several determined influencing factors related to seismically triggered landslides inventory. This assessment is to analyze which factors have the most positive correlation quantitatively.

Several studies have been carried out on landslides triggered by an earthquake in Indonesia regions (**Wang et al., 2011; Ueno and Shiiba, 2013; Faris and Wang, 2014; Resfiandhi et al., 2014; Nakano et al., 2015; Resfiandhi et al., 2015; Sumaryono et al., 2015; Zhao, 2021**), with only a few related to susceptibility assessment (**Umar et al., 2014; Sumaryono et al., 2015; Saputra et al., 2016; Hadi et al., 2018; Sadisun et al., 2021**). In an earthquake-prone area, identifying the susceptibility to landslides is crucial to develop and implementing disaster management for future occurrences by providing susceptibility mapping in particular. The Ministry of Agrarian Affairs and Spatial Planning/National Land Agency of Indonesia following the 2018 earthquake disaster prioritized disaster-based spatial planning in the area covered in this study (**Andiani et al., 2018**). This paper provides a practical method for susceptibility assessment of earthquake-induced landslides, and the result, a thematical map, contributes to post-earthquake disaster recovery.

2. Geological setting

The city of Palu is the capital of the Central Sulawesi Province, Indonesia, located in the plains of the Palu Valley and Palu Bay (see **Figure 1A**). Morphologically, the area is divided into five landscapes: mountains, valleys, rivers, bays, and oceans. The area of Palu reaches 395.06 square kilometers, divided into eight districts. Geographically, Palu is between 0°,36”-0°,56” South Latitude and 119°,45” – 121°,1” East Longitude, so it is right on the Equator with an altitude of 0-700 meters above sea level. Palu's topography is shaped by the movement of the left-lateral strike-slip PKF, with a gentle sloping in the alluvium fan area that spreads to the volcanic foot slopes of the pre-tertiary and tertiary mountains, high up to 2,000 m ASL altitude (**Socquet et al., 2019; Syifa et al., 2019**).

Palu is a small part in the northwest of Sulawesi Island, situated on the junction of three major tectonic plates; the Eurasian, Pacific, and Indian - Australian plates. The complex evolution of its motion and series of displacements resulted in a distinctive fault system, the PKF (**Walpersdorf and Vigny 1998**). This period was accompanied by phases of magmatism and metamorphism (**Bergman et al., 1996; White et al., 2017; Socquet et al., 2019**). This composed the valley region and the surrounding areas
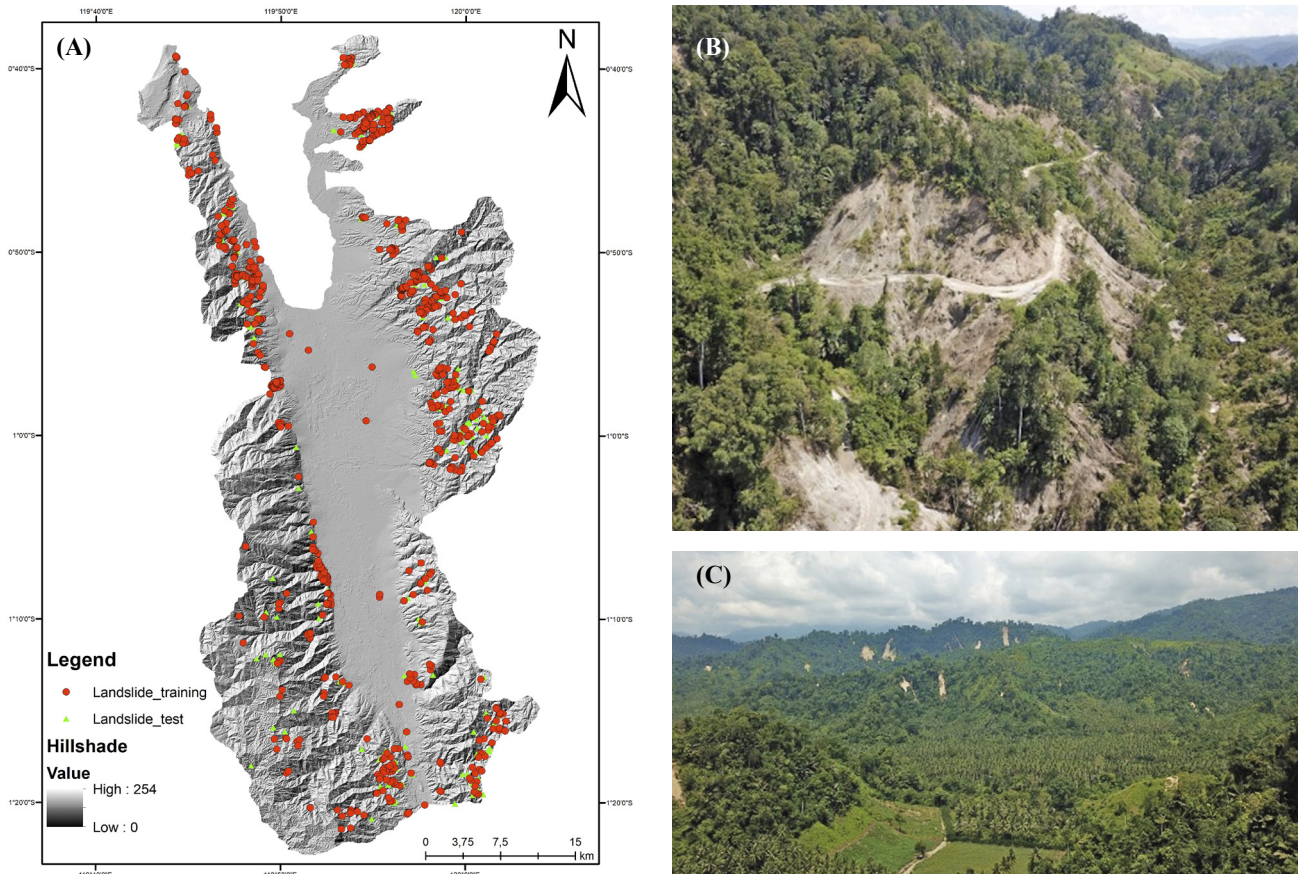
Figure 2: (A) Landslide inventory map; **(B)** Aerial photo of coseismic landslides in Sigi Regency, the southern part of the study area; **(C)** Landslides in Donggala Regency, the northern part of the study area.

with pre-tertiary, tertiary, and quaternary rocks. It is dominated by several metamorphic core complexes overlain by volcanic and quaternary sedimentary deposits, magmatic intrusions, and complex rock units (**van Leeuwen et al., 2016**). Overall, the stratigraphic structure of the city of Palu is composed of three rock groups, namely: Pre-Tertiary rock groups, Tertiary rock groups, and Quaternary rock groups. The Pre-Tertiary rock can be found in the form of marine sedimentary rocks and metamorphic, both of which are intruded Tertiary-aged granite and granodiorite and unconformably overlain by the Quaternary group, which consists of several deposits, namely: debris deposits, river deposits, flood-abundant deposits, ancient river channel deposits, and alluvium fan deposits. Beach deposits in the form of beach sand and rock fragments are often found around Palu Bay (**Simandjuntak et al., 1991; Hall and Wilson, 2000; van Leeuwen and Muhardjo, 2005; Watkinson, 2011; Marjiyono et al., 2013**).

3. Data

Landslide inventory is the initial and compulsory data for landslide susceptibility assessment (LSA) (see **Figure 2A**), represented in a spatial distribution mapping (**Fell et al., 2008; Galli et al., 2008; van Westen et al., 2008; Zieher et al., 2016; Arifianti and Agustin, 2017**).

Landslide inventory in this study solely compiled the events that occurred within and promptly after the ground shaking (coseismic landslides). A total of 1273 landslide points in this area were displayed in the landslide inventory map. Landslides triggered by the Palu earthquake are mostly classified as rockfalls, rock slides, soil slides, and their combination. Historically, rockfalls and rock slides are the most prolific landslide types triggered by earthquakes globally (**Keefer, 2002; Jibson et al., 2006**). This area is close to the earthquake source. Along the PKF path, in the southern part of the study area, the slope failures mostly consist of rock and soil slides (see **Figure 2B**). A combination of slides and rockfalls occurs in the northern part of the Donggala area (see **Figure 2C**). (**Sumaryono et al., 2018**).

After constructing the event-based landslide inventory, the next step is processing a dataset of the relevant causative factors. Causative factors are predisposing factors, some functions of direct and indirect natural and human influence, determining landslide trigger factors (**van Westen, 2000**). The causative factors are lithology, land use, slope gradient, aspect, elevation, and peak ground acceleration (PGA). The six appointed data factors were selected based on the study developed by **Sidle and Ochiai (2006)**. The factors related to earthquake features, as in PGA and the others, are relevant to the environment in which the earthquake is recurring.

The distribution of the landslide events was closely associated with the topographic attributes, such as slope (gradient and aspect) and elevation. For instance, in the course of an earthquake event, ground tremors escalate as elevation raises (**Sepúlveda et al., 2005; Zhou et al., 2016**). Slope gradient represents levels of the steepness of land surfaces since the driving force of a landslide is gravity. The slope aspect is the direction of the land surface and presents a vital function in slope stability. The slope becomes unstable due to the variation in temperature, vegetation, and direction of PGA (**Dou et al., 2015**). It relates to weather elements (sunlight exposure, temperature, winds, precipitation) which control the soil moisture and strength (**Galli et al., 2008; Capitani et al., 2014**).

Specific land use types can control slope stability, e.g. disturbed slope due to road construction and settlements, land use shifting from forested areas to cultivation/agricultural purposes. Hence, it will significantly increase the potential of landslide events (**Reichenbach et al., 2014; Meneses et al., 2019**).

Lithology, as the key parameter in LSA, defines the variety of geological units or rock formations that determine the topography's geo-mechanical features. Every unit has individual characteristics, deriving a distinctive resistance on each unit to ground motion (**Torizin, 2011; Costanzo et al., 2012; Gautam et al., 2021**).

PGA was studied as the focal mark of an earthquake, as well as a dynamic parameter in the assessment of earthquake-induced landslides. The tremor will generate an extra burden on a slope, amplifying the pore water pressure in the previously saturated water slopes, thus intensifying the driving force on the slope (**Zhou, 2016**). **Meunier et al. (2007)** mentioned in their findings that the density of post-seismic landslides culminated where ground accelerations were the largest.

4. Methods

Landslide inventory was collected using Remote Sensing (RS) data interpretation and a ground-based field survey throughout the Palu area and the surroundings of approximately 1731 km² promptly following the earthquake. High-resolution aerial imageries of 0.6 m for landslides are accumulated by using an Unmanned Aerial Vehicle (UAV) tool. The earthquake-damaged area images were taken in the post-disaster phase by several state institutions, Geospatial Information Agency/ BIG, Geological Agency/BGL, Meteorology, Climatology, and Geophysical Agency/BMKG. Multiple ground-based checking coincides with other RS surveys done by BGL (**Sumaryono, et al., 2018**) to construct an inventory map.

The landslide data were obtained in a short time during the disaster emergency response period, where some of the landslide's characteristics (i.e. type, size, volume, etc.) are not comprehensively documented by the field survey team (**Sumaryono, et al., 2018**). Therefore, the data are outlined as geospatial-based points to construct a homogeneous database pinpointed nearby the scar of the landslide body (**Neuhäuser, et al., 2011; Silalahi, et al., 2019**). The data was divided into two data series. To be sufficiently representative, we used a 70:30 ratio, 70 is used to execute the model and the rest is for model validation (**Zhou, et al., 2016; Silalahi, et al., 2019; Saha, et al., 2020; Ikram, et al., 2023**). The partition of the landslide was completed using the tool titled "Subset Features" in ArcGIS.

4.1. Landslide and causative factors

The 1273 landslides were divided into two data series; 70% points as training data (891 events) were elected for designing the landslide susceptibility model. The 30% points as test data (382 events) were selected for model validation purposes. Then, each of the six causative factors was rasterized with a cell size of 7.5 x 7.5 m grid and reclassified it into various sub-classes.

The topographical features were acquired using a 7.5 m resolution of the Digital Elevation Model (DEM) from the TerraSAR-X satellite data. The features include elevation, slope gradient, and slope aspect. The slope gradient was classified into seven units based on the slope classification of the U.S. Department of Agriculture, as follows: flat (< 2°), undulating (2–5°), moderately sloping (5–8°), hilly (8–17°), moderately steep (17–24°), steep (24–33°), and very steep (> 33°) (**Pamela, et al., 2018**). The slope aspect was redivided into nine classes and the elevation was classified into 12 units, as seen in **Table 1**.

Land use and lithology factors are secondary data. Land use maps were acquired from the BIG. Land use classification is based on the Indonesian Standard Land Cover Classification standardized by the National Standardization Agency/BSN in 2010 (**Nurwadjedi et al., 2015**). The lithology map was provided from the geology map of 1: 50,000 scale (see **Figure 1B**), modified by the Geological Survey Institute/PSG, formerly known as the Geological Research and Development Centre. Ten categories of land use were identified as settlement, open land, sand landscape, forest (high land and low land), bush and scrubs, mangrove forest, plantation forest, rice fields (seasonal wetland agriculture), agriculture (seasonal dry land agriculture), and river. The lithology map consists of 10 types, as presented in **Figure 1B**.

Deterministic seismic hazard analysis (DSHA) is carried out to calculate the estimated PGA in Palu. Modelling was done using OpenQuake software developed by the Global Earthquake Model (GEM). The earthquake parameters in this modelling are taken from the GFZ moment tensor solution (**GFZ, 2018**). The PGA map was defined into 10 classes, extending from 0 to 0.54.

The geometry of the fault line for the Palu earthquake is taken from the Indonesian Earthquake Source and

Hazard Map 2017 (**Pusgen, 2017**) which was modified by the BGL emergency response team assigned to Palu right after the earthquake. The calculation of the PGA utilizes three ground motion prediction equations (GMPEs), namely: **Boore et al. (2014)**, **Campbell and Bozorgnia (2014)**, and **Chiou and Youngs (2014)** with their respective weights 1/3. These three attenuation equations are intended to overcome the epistemic uncertainties that arise because there is no inherent GMPE based on earthquake shock data in Indonesia. The modelling result of the Mw 7.5 Palu earthquake on bedrock shows that most episodes of ground shaking are found in the area closest to the fault line, which reaches 0.4 - 0.45 g. The ground shaking decreases as it moves further away from the fault line.

4.2. Landslide susceptibility analysis

One bivariate statistical method, weights of evidence (WoE), was implemented to analyze landslide susceptibility. WoE is a variant of log-linear in the Bayes postulate used to quantify the probability (P) centered on the idea of prior and posterior P (**Elmoulat et al. 2015**). The input data for this model acted as landslide causative factors, were the source information which may cause the areas susceptible to landslides. The spatial correlation which linked the causative factors (VP) and the distribution of landslides (VM), was estimated as weights by this method in the shape of positive (W+) and negative (W-). These weights were assessed from the natural logarithm's ratios (**Equations 1** and **2**) (**Elmoulat et al., 2015**).

$$W+ = \ln \frac{P\{VP/VM\}}{P\{VP/\overline{VM}\}} \qquad (1)$$

$$W- = \ln \frac{P\{\overline{VP}/VM\}}{P\{\overline{VP}/\overline{VM}\}} \qquad (2)$$

The analysis stages can be compiled shortly as follows (**Sinčić et al., 2022**): (1) landslide data collection, then divided into training data and test data; (2) extraction of landslide causative data and computation of the weights with training data; (3) estimation of all causative data to forecast the probable landslide events; (4) applying test data into validation process.

The last step, the validation process to verify how good the model is, uses the Area Under the Curve (AUC) of the Receiver Operating Characteristic (ROC). It was done by measuring the susceptibility maps with a pair of landslide data, creating two rate curves, success rate and prediction rate. The success rate depicted the accuracy of the current landslides, while the prediction rate showed the performance of the submitted landslide model for predicting landslide susceptibility (**Chung and Fabbri, 2003**). The model quality will be considerably more accurate if the

Table 1: The weight of evidence for classes of each causative factor

| Classes of Factor	Class Pixels	Land-slide	W+	W-	WFinal
Slope gradient (degree)					
< 2	34352	10	-2.24	0.10	-2.52
2 – 5	49941	10	-2.61	0.16	-2.94
5 – 8	23855	12	-1.70	0.06	-1.94
8 – 17	53273	63	-0.85	0.11	-1.13
17 – 24	44735	106	-0.15	0.02	-0.35
24-33	62595	230	0.29	-0.08	0.20
>33	53624	459	1.14	-0.54	1.51
Slope Aspect					
Flat	47444	56	-2.94	0.09	-3.06
N	33172	97	-2.03	-0.01	-2.05
NE	33132	150	-1.59	-0.07	-1.54
E	32328	221	-1.18	-0.17	-1.02
SE	30267	154	-1.47	-0.09	-1.41
S	35183	48	-2.79	0.06	-2.88
SW	40170	47	-2.95	0.07	-3.05
W	40537	54	-2.82	0.07	-2.91
NW	30142	63	-2.37	0.02	-2.42
Elevation (m)					
0-200	132134	125	-1.07	0.38	-1.45
200–400	44312	301	0.90	-0.27	1.17
400-600	34240	265	1.04	-0.24	1.27
600-800	31170	103	0.18	-0.02	0.20
800-1000	28442	42	-0.63	0.04	-0.67
1000-1200	23426	33	-0.67	0.04	-0.71
1200-1400	14921	13	-1.15	0.03	-1.19
1400-1600	6427	6	-1.08	0.01	-1.10
1600-1800	3428	1	-2.24	0.01	-2.25
1800-2000	2422	1	-1.90	0.01	-1.91
2000-2200	1448	0	-6.80	0.00	-6.80
2200-2400	5	0	-6.80	0.00	-6.80
Land use					
Settlement	17711	3	-2.78	0.05	-2.99
Open Land	431	0	-6.80	0.00	-6.95
Sand	374	0	-6.80	0.00	-6.95
Forest	130839	480	0.28	-0.25	0.38
Bush	75299	315	0.42	-0.17	0.43
Mangrove	5	0	-6.80	0.00	-6.95
Plantation	26487	4	-2.89	0.08	-3.13
Rice fields	19542	1	-3.93	0.06	-4.15
Agriculture	50158	87	-0.47	0.07	-0.69
River	1529	0	-6.80	0.00	-6.96
Lithology unit					
Qp	53217	211	0.36	-0.09	0.40
Qa	98171	19	-2.65	0.34	-3.04
Tmpl	27819	86	0.11	-0.01	0.07
Tpkg	682	0	-6.80	0.00	-6.85
Tt	10839	56	0.63	-0.03	0.61
Tmpi	89875	385	0.44	-0.24	0.63
Qtms	9162	13	-0.67	0.01	-0.73
Kls	31684	120	0.32	-0.04	0.31
Trw	448	0	-6.80	0.00	-6.85
TRjgg	478	0	-6.80	0.00	-6.85
PGA					
0-0.21	31813	20	-1.48	0.08	-1.60
0.21-0.24	35959	78	-0.24	0.03	-0.31
0.24-0.28	29623	180	0.79	-0.13	0.88
0.28-0.32	30721	47	-0.59	0.05	-0.68
0.32-0.35	25755	101	0.35	-0.04	0.35
0.35-0.39	31955	70	-0.23	0.02	-0.29
0.39-0.43	29359	37	-0.78	0.05	-0.88
0.43-0.47	30162	36	-0.84	0.06	-0.94
0.47-0.50	32622	67	-0.30	0.03	-0.36
0.50-0.54	44406	254	0.73	-0.19	0.88
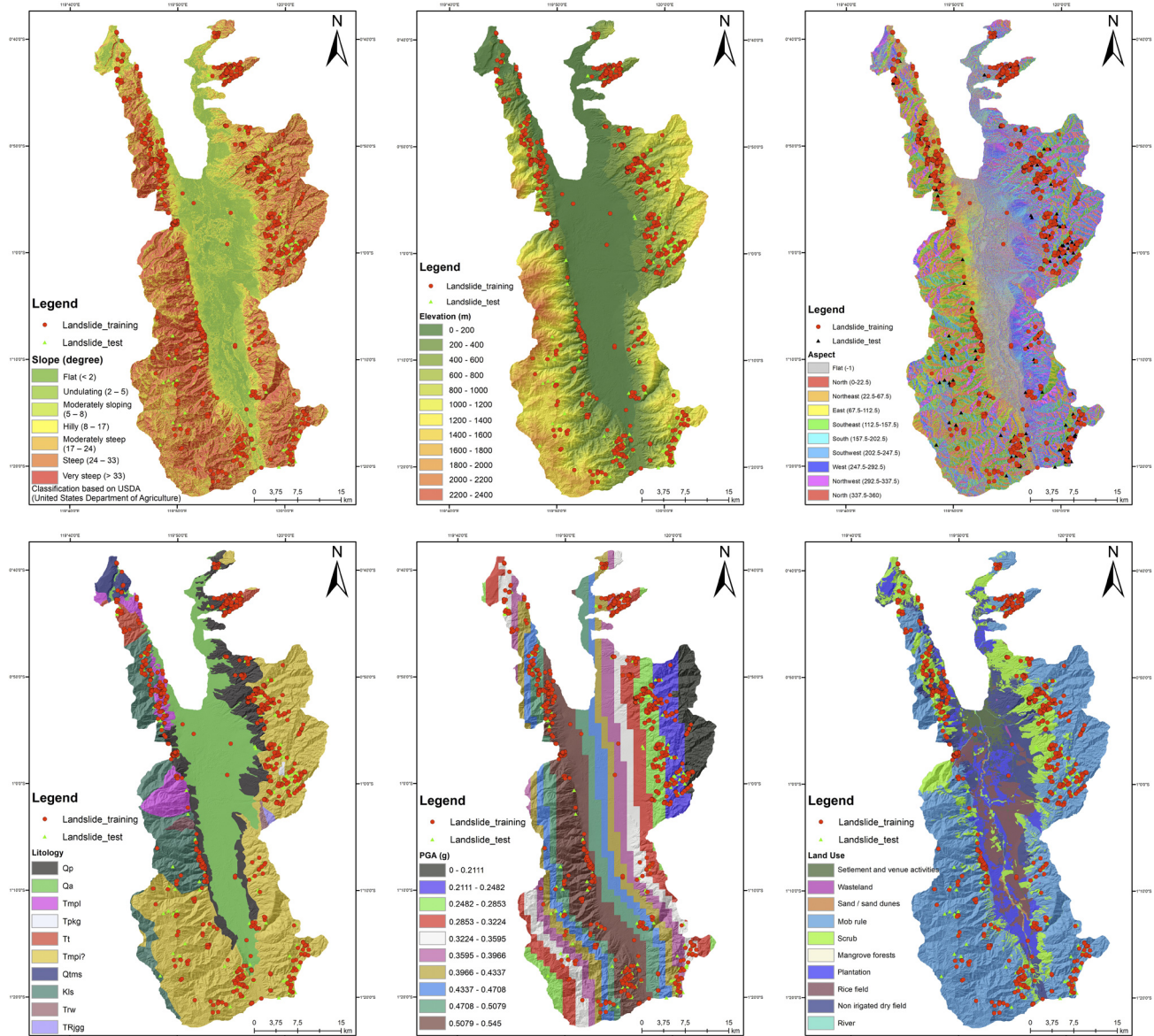
Figure 3: The causative factors combined with landslides distribution; **(A)** slope gradient; **(B)** elevation; **(C)** slope aspect; **(D)** lithology unit; **(E)** PGA; and **(F)** land use

AUC value is close to 1.0 (**Chung and Fabbri, 2003; Pourghasemi et al., 2013**).

5. Results and Discussion

The list of all data (causative factors) and the corresponding classes, including the WoE calculated spatial interrelation between the landslide points in the area with the causative factors were illustrated in **Table 1** and **Figure 3**.

The most positive value between slope gradient and landslides shows that the slope degree of 24°-33° and >33° is the highest susceptible to landslides, with 54% occurrences of the total landslide. This outcome is expected because slope failures resulting in landslide activation are associated with severe slope areas (> 30) (**Tang, et al., 2011; Yang, et al., 2015; Çellek, S.,**

2020a). However, a small number of landslides (≈ 2%) occurred in flat to moderate sloping areas (< 8°). In this case, a massive flow slide was developed during the earthquake-induced liquefaction in an alluvial fan deposit on a denudational slope near Palu Bay (**Cilia, et al., 2021; Jalil, et al., 2021; Tohari, A. et al., 2022**). Aside from that, the slope along the riverbanks in the plain geomorphic conditions is also prone to seismically triggered landslides (**Hu et al., 2021; Wubalem, 2021**).

As for the slope aspect, the three classes with the least negative value are in the east (E), northeast (NE), and southeast (SE) directions. Those are the most susceptible to landslides, with 525 recorded events (≈ 41%). This corresponds with several studies that stated the east–south-facing slopes are very susceptible to mass failures because they are affected by slope exposure to the sun, intense wetting, moisture during the rainy season, and
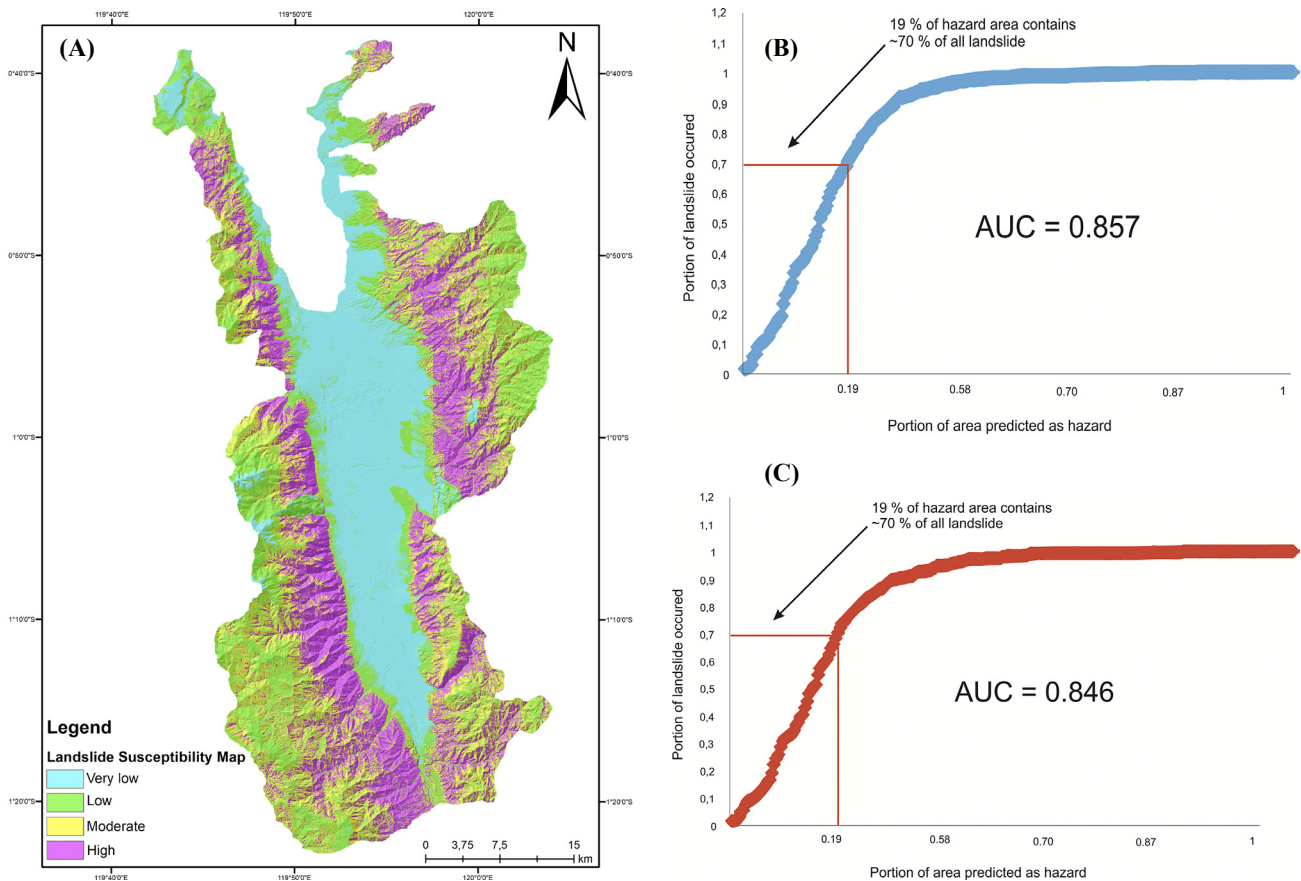
Figure 4: (A) Landslide susceptibility map produced using WoE method; **(B)** Success rate curve and, **(C)** the Prediction rate curve represents the quality of the model.

drying cycles (**Capitani et al., 2014**; **Masoumi et al. 2014**; **Mandal and Mandal, 2016; Çellek, S., 2021**).

The region, located from 200 to 600 meters above sea level (asl), is subjected to an excessive quantity of landslides (566 points). This is possible since the study area is primarily positioned along the 0 – 800 m asl. Relevant studies stated a correlation between elevation to seismic-triggered landslide at higher or lower altitudes (**Bai et al., 2014**; **Tanoli et al. 2017**; **Çellek S., 2020b**). In this study, the seismic motion stimulates most landslides in the lower elevation, which is aligned with the orientation of the PKF line (**Çellek S., 2020b**).

The land use factor produces a distinctive result, congruent with **Kamp et al. (2008)** and **Teerarungsigul et al. (2015)** study, where the landscape of the survey area covered by forested and brush/scrub land presents a positive outcome on landslide activity. Both account for nearly 90 percent of landslide occurrences. This is reasonable, the survey area is significantly overlaid by about 64% by both classes. **Teerarungsigul et al. (2015)** believed that the forest class corresponds remarkably with steeper slopes, which frame a first-rate importance parameter for landslide incidents. **While Kamp et al. (2008)** assumed that the shrubland (brush/scrubland) in some sections of the study area portrays a succession phase after preliminary deforestation.

The uppermost percentage of landslides in the lithology class can be found in the Latimojong Formation (Tmpi), which is composed of metamorphosed rocks, slate, phyllite, chert, marble, quartzite, and silicified breccia, with a few oldest rocks of greywacke, limestone, argillite and siltstone with conglomeratic intercalations. This study and other research (**Igwe, 2015**) on landslide susceptibility assessment proved that metamorphic rocks have a high susceptibility to landslides. The presumption in the Palu area, which is covered by metamorphic mass, is highly affected by the weathering process, which gradually weakened the material strength, and evidence of shear surfaces creating ruptures, cracks, and deformations on slope surfaces which subsequently initiated the slope failure (**Parkash, 2011**; **5**; **Teerarungsigul et al., 2015; Gautam et al., 2021**). Similar cases associated with earthquake-induced landslides study demonstrate that the exposed area is on steeper slopes at high elevations as a result of fault movement, in this case, PKF, which caused intense fracturing, thus related to high seismicity (**Schlagel et al., 2016**). Another comparable fact from **Kamp et al. (2008)**, metamorphic rocks have proven to be the highest landslide, with most of the landslides occurring along faults.

The highest positive correlation between PGA and landslides is located in the range of 0.5 g to 0.54 g. This

corresponds with the modelling result on bedrock, where the highest ground shaking is found in the area closest to the fault line at 0.4 - 0.45 g. The same positive value is seen at 0.24-0.28 g, spatially, it is on the natural slope near the earthquake source. A few studies focused on the relationship between PGA and earthquake-triggered landslides. **Ademović (2017)** analyzed 24 cases and found that predominantly the landslide-affected areas are located in the range of 0.5 g to 1.2 g. **Ghahramani (2012)** concluded that from the 18 calculated events, 12 of them were situated in the range of 0.21 g to 0.62 g. **Wang et al. (2010)** observed that landslides induced by the earthquake are mostly clustered in the area with a PGA > 2 m/s^2 (> 0.204 g). **Parkash (2011)** remarks in his study that the PGA range of 0.25 g up to 0.4 g was resulting from the acceleration of ground shaking that can generate landslides in hillslopes.

The AUC of the success rate of slope gradient, slope aspect, elevation, land use, lithology, and PGA are 0.768, 0.681, 0.734, 0.645, 0.677, and 0.668, respectively. It indicates that the topographic features are the top three significant factors controlling the incidence of landslides in this study area. This is predictable due to the precision of the parameter input originating from high-quality DEM. Moreover, the slight differences in the AUC value between the parameter implied that the computed input data are approved, i.e. the landslide quantity, the selected scale, and the resolution. The validation results of the causative factors demonstrate how good the correlation between the factors and the earthquake-induced landslides is.

The WoE technique applied to the training data series produced earthquake-induced landslides in the Palu area, Indonesia (see **Figure 4A**). The success rate lies at 85.7%, while the prediction rate stands at 84.6% of accuracy (see **Figures 4B** and **4C**). The curve supplies a basis to differentiate the susceptibility levels, which were sorted into four susceptibility zones, (1) very low; (2) low; (3) moderate; and (4) high landslide susceptibility (see **Figure 4A**). The zonation of landslide susceptibility and the colour combination is based on the Indonesian National Standard (SNI) titled the Preparation and Specification of Landslide Susceptibility Zonation (**BSN, 2016**).

64% of the evidenced landslides were identified in the areas with moderate and very high susceptibility levels. The remaining percentage is divided into low and very low susceptibility. Clustered landslides in a very low zone are associated with liquefaction events and riverbank slope failures in a gentle slope.

Similar research studies include matching input data (related factors) and chosen methods (statistical) also producing accurate susceptibility products in their area of interest, with a success rate and good prediction accuracy of >70% (**Dou, et al., 2015; Silalahi, et al., 2019; Xu, et al., 2021; Fan, et al., 2023; Zhao, et al., 2023**). Hence, the specified model is relatively capable to produce a reliable landslide susceptibility map.

6. Conclusions

A quantitative method of the weight of evidence model was conducted to assess the relation between landslides and six causative factors, i.e. lithology, land use, peak ground acceleration, slope gradient, aspect, and elevation to determine the susceptibility level, and to derive an earthquake-induced landslide susceptibility map in Palu and the surrounding areas in Indonesia. The estimated success rate is 85.7%, which shows that the model's relevancy is good with the occurrence of landslides. The prediction rate is 84.6% indicating the applied model is very good at predicting successive landslides.

Aside from the favourable result, this study proposed an event-based susceptibility mapping of earthquake-induced landslides. The generated susceptibility map is subject to revision. The LSM can be enhanced for further assessment by including additional landslide causative factors. The subsequent mapping could also use more comprehensive landslide categories, taken from historical records and post-seismic landslides. This notably simple method can be a practical tool for the rapid assessment of reconnaissance research in the neighbouring area of Palu, or other regions in Indonesia, which are susceptible to earthquake-induced landslides. It provides a baseline for another novel earthquake-induced landslide study. Additionally, producing an earthquake-induced LSM substantially contributes to land use-spatial planning in the Palu region and the surrounding areas, as one of the non-structural measures of disaster management.

7. References

Ademović, N. (2017): High magnitude earthquakes trigger landslides and floods. In: the Geoexpo the 7th Scientific and Expert Conference on Geotechnics, Sarajevo, October 26-27, 2017. doi: 10.35123/GEO-EXPO_2017_18.

Andiani, Yuwana, D. A., Firdaus, E. R., Andrikni, W. K. M., Kurniah, H., and Taufiq, W. B. (2018): Geological Based Spatial Planning. In: Andiani, Oktariadi O., Kurnia A. (eds) Di Balik Pesona Palu. Badan Geologi, 201-213. (*in Bahasa*)

Arifianti, Y., and Agustin, F. (2017): An Assessment of the Effective Geofactors of Landslide Susceptibility: Case Study Cibeber, Cianjur, Indonesia. In: Yamagishi H., Bhandary NP. (eds) GIS Landslide. Springer Japan KK, 183-195.

Bai, S.B., Wang, J., Thiebes, B., Cheng, C., and Chang, Z.Y. (2014): Susceptibility assessments of the Wenchuan earthquake-triggered landslides in Longnan using logistic regression. Environmental Earth Sciences 731–743.

Bellier, O., Sebrier, M., Beaudouin, T., Villeneuve, M., Braucher, R., Bourles, D., Siame, L., Putranto, E., and Pra-

tomo, I. (2001): High slip rate for a low seismicity along the Palu-Koro active fault in central Sulawesi (Indonesia). Terra Nova, 13, 463-470. https://doi.org/10.1046/j.1365-3121.2001.00382.x.

Bergman, S.C., Coffield, D.Q., Talbot, J.P., and Garrard, R.A. (1996): Tertiary Tectonic and magmatic evolution of western Sulawesi and the Makassar Strait, Indonesia: evidence for a Miocene continent-continent collision. Geo Soc London Spec Publ, 106, 391-429. https://doi.org/10.1144/GSL.SP.1996.106.01.25.

BNPB, (2019): Infografis gempabumi M7,4 dan tsunami Sulawesi Tengah update 5 Febuari 2019, pukul 20.00 WIB. https://bnpb.go.id/publikasi/infografis/infografis-gempabumi-m74-tsunami-sulawesi-tengah.html Accessed 21 June 2019.

Boore, D.M., Stewart, J.P., Seyhan, E., and Atkinson, G.M. (2014): NGA-West2 equations for predicting PGA, PGV, and 5% Damped PSA for shallow crustal earthquakes. Earthquake Spectra, 30(3), 1057-1085.

BSN. (2016). SNI 8291:2016 Preparation and Specification of Landslide Susceptibility Zonation. Badan Standardisasi Nasional (BSN) Jakarta, Indonesia. (*in Bahasa*)

Campbell, K.W., and Bozorgnia, Y. (2014): NGA-West2 ground motion model for the average horizontal components of PGA, PGV, and 5% Damped Linear Acceleration Response Spectra. Earthquake Spectra, 30(3), 1087-1115.

Capitani, M., Ribolini, A., and Bini, M. (2014): The slope aspect: a predisposing factor for landsliding. CR Geoscience,106, 391-429.

Çellek, S. (2020a): Effect of the Slope Angle and Its Classification on Landslide, Nat. Hazards Earth Syst. Sci. Discuss. [preprint], https://doi.org/10.5194/nhess-2020-87

Çellek, S. (2020b): Morphological parameters causing landslides: A case study of elevation. Bulletin of the Mineral Research and Exploration 162, 197-224. https://doi.org/10.19111/bulletinofmre.649758

Çellek, S. (2021): The Effect of Aspect on Landslide and Its Relationship with Other Parameters. In: Zhang Y., Cheng Q. (eds) Landslide. IntechOpen, 2. https://doi.org/10.5772/intechopen.99389

Chiou, B.S.J., and Youngs, R.R. (2014): Update of the Chiou and Youngs NGA model for the average horizontal component of Peak Ground Motion and response spectra. Earthquake Spectra, 30(3), 1117-1153.

Chung, C.J.F., and Fabbri, A.G. (2003): Validation of spatial prediction models for landslide hazard mapping. Nat Haz, 30(3), 451–472.

Cilia, M.G., Mooney, W.D., and Nugroho, C. (2021): Field Insights and Analysis of the 2018 Mw 7.5 Palu, Indonesia Earthquake, Tsunami and Landslides. Pure Appl. Geophys. 178, 4891–4920. https://doi.org/10.1007/s00024-021-02852-6.

Costanzo, D., Rotigliano, E., Irigaray, C., Jiménez-Perálvarez, J.D., and Chacón, J. (2012): Factors selection in landslide susceptibility modelling on large scale following the gis matrix method: application to the river Beiro basin (Spain). Nat Hazards Earth Syst Sci, 12, 327–340. doi: 10.5194/nhess-12-327-2012.

Dou, J., Tien Bui, D., Yunus, A.P., Jia, K., Song, X., Revhaug, I., Xia, H., and Zhu, Z. (2015): Optimization of Causative Factors for Landslide Susceptibility Evaluation Using Remote Sensing and GIS Data in Parts of Niigata, Japan. PLoS ONE, 10(7), e0133262.https://doi.org/10.1371/journal.pone.0133262.

Elmoulat, M., Brahim, L. A., Mastere, M., and Jemmah, A. I. (2015): Mapping of Mass Movements Susceptibility in the Zoumi Region Using Satellite Image and GIS Technology (Moroccan Rif) . International Journal of Scientific & Engineering Research 6 210-217

Fan, X., Liu, B., Luo, J., Pan, K, Han, S., and Zhou, Z. (2023): Comparison of earthquake-induced shallow landslide susceptibility assessment based on two-category LR and KDE-MLR. Sci Rep 13, 833. https://doi.org/10.1038/s41598-023-28096-z

Faris, F.W., and Fawu, W. (2014): Investigation of the initiation mechanism of an earthquake-induced landslide during rainfall: a case study of the Tandikat landslide, West Sumatra, Indonesia. Geoenvironmental Disasters, 1, 1-18.

Fell, R., Corominas, J., Bonnard, C., Cascini, L., Leroi, E., and Savage, W.Z. (2008): Guidelines for landslide susceptibility, hazard and risk zoning for land-use planning. Eng Geol, 102, 85–98.

Galli, M., Ardizzone, F., Cardinali, M., Guzzetti, F., and Reichenbach, P. (2008): Comparing landslide inventory maps. Geomorphology, 94(3-4), 268-289. https://doi.org/10.1016/j.geomorph.2006.09.023.

Gautam, P., Kubota, T., and Aditian, A. (2021): Evaluating underlying causative factors for earthquake-induced landslides and landslide susceptibility mapping in Upper Indrawati Watershed, Nepal. Geoenviron Disasters 8, 3. https://doi.org/10.1186/s40677-021-00200-3.

GFZ. (2018): Moment tensor solution. https://geofon.gfz-potsdam.de/eqinfo/event.php?id=gfz2018tabt Accessed 10 October 2018.

Ghahramani, M. (2012): Coupling of two natural complex systems: earthquake-triggered landslides. Master thesis, University of Waterloo, Ontario, Canada.

Go´mez, J.M., Madariaga, R., Walpersdorf, A., and Chalard, E. (2000): The 1996 earthquakes in Sulawesi, Indonesia. Bull Seism Soc Am, 90(3), 739–751.

Hadi, A.I., Brotopuspito, K.S., Pramumijoyo, S., and Hardiyatmo, H.C. (2018): Regional landslide potential mapping in earthquake-prone areas of Kepahiang Regency, Bengkulu Province, Indonesia. Geosciences, 8(6), 219 https://doi.org/10.3390/geosciences8060219.

Hall, R., and Wilson, M.E.J. (2000): Neogene Sutures in Eastern Indonesia. Journal of Asian earth Sciences, 18, 781-808.

Hu, M., Wu, Z., Reicherter K., Ali, S., Huang, X., and Zuo, J. (2021): A Historical Earthquake-Induced Landslide Damming Event at the Qiaojia Reach of the Jinsha River, SE Tibetan Plateau: Implication for the Seismic Hazard of the Xiaojiang Fault. Front. Earth Sci. 9:649543. doi: 10.3389/feart.2021.649543.

Igwe, O. (2015): The geotechnical characteristics of landslides on the sedimentary and metamorphic terrains of South-East Nigeria, West Africa. Geoenvironmental Disasters, 2(1).

Ikram, R.M.A., Dehrashid, A.A., Zhang, B., Chen, A., Le, B. N., and Moayedi, H. (2023). A novel swarm intelligence: cuckoo optimization algorithm (COA) and SailFish optimizer (SFO) in landslide susceptibility assessment. Stoch Environ Res Risk Assess 37, 1717–1743 (2023). https://doi.org/10.1007/s00477-022-02361-5.

Jalil, A., Fathani, T.F., Satyarno, I., and Wilopo, W. (2021): Liquefaction in Palu: the cause of massive mudflows. Geoenviron Disasters 8, 21. https://doi.org/10.1186/s40677-021-00194-y.

Jibson, R.W., Harp, E.L., Schulz, W., and Keefer, D.K. (2006): Large rock avalanches triggered by the M-7.9 Denali Fault, Alaska, earthquake of 3 November 2002. Engineering Geology, 83, 144–160.

Kamp, U., Growley, B. J., Khattak, G. A., and Owen L. A. (2008): GIS-based landslide susceptibility mapping for the2005 Kashmir earthquake region. Geomorphology 101:631–642 (13).

Keefer, D.K. (2002): Investigating landslide caused by earthquakes-a historical review. Surveys in Geophysics, 23, 473–510.

Mandal, B., and Mandal, S., (2016): Assessment of mountain slope instability in the Lish River basin of Eastern Darjeeling Himalaya using frequency ratio model (FRM). Model. Earth Syst. Environ, 2, 121. https://doi.org/10.1007/s40808-016-0169-8.

Marjiyono, Kusumawardhani, H., and Soehaimi, A. (2013): Struktur geologi bawah permukaan dangkal berdasarkan interpretasi data geolistrik, studi kasus sesar Palu Koro. JSD Geol, 23, 39–45.

Masoumi, H., Jamali, A.A., and Khabazi, M. (2014): Investigation of Role of Slope, Aspect and Geological Formations of Landslide Occurrence Using Statistical Methods and GIS in Some Watersheds in Chahar Mahal and Bakhtiari Province. Model. J. Appl. Environ. Biol. Sci., 4(9), 121-129.

Meneses, B.M., Pereira, S., and Reis, E. (2019): Effects of different land use and land cover data on the landslide susceptibility zonation of road networks. Nat. Hazards Earth Syst. Sci., 19, 471–487. https://doi.org/10.5194/nhess-19-471-2019.

Meunier, P., Hovius, N., and Haines, A.J. (2007): Regional patterns of earthquake-triggered landslides and their relation to ground motion. Geophysical Reseaarch Letters, 34(20), L20408. https://doi.org/10.1029/2007GL031337.

Nakano, M., Chigira, M., Lim, C.S., and Sumaryono. (2015): Geomorphological and geological features of the collapsing landslides induced by the 2009 Padang earthquake. In: Proceedings of 10th Asian Regional Conference of IAEG on "Geohazards and Engineering Geology", Kyoto, Japan, 26-29 September, 2015.

Neuhäuser, B., Damm, B., and Terhorst, B. (2011): GIS-based assessment of landslide susceptibility on the base of the weights-of evidence model. Landslides, 9, 511–528.

Nurwadjedi, Suprajaka, and Sampurno, D.T.W. (2015): Developing national geospatial Thematic information on land cover/land use: an implementation of One Map Policy. Paper presented at FIG Working Week 2015, From the Wisdom of the Ages to the Challenges of the Modern World, Sofia, Bulgaria, 17-21 May 2015.

Pakpahan, S., Ngadmanto, D., Masturyono, Rohadi, S., Rasmid, Widodo, H.S., and Susilanto, P. (2015): Seismicity analysis in Palu Koro Fault Zone, Central Sulawesi. J. Environ. Geol. Haz, 6, 253–264.

Pamela, Arifianti, Y., Sadisun, I. A., and Kartiko, R. D. (2018): The selective causative factors on landslide susceptibility assessment: Case study Takengon, Aceh, Indonesia. In: AIP Conference Proceedings 1987(1):020089. https://doi.org/10.1063/1.5047374

Parkash, S. (2011): Earthquake Related Landslides in the Indian Himalaya: Experiences from the Past and Implications for the Future. In: Proceedings of the Second World Landslide Forum, Rome, Italy, 3-7 October 2011.

Pourghasemi, H.R., Moradi, H.R., and Aghda, F.S.M. (2013): Landslide susceptibility mapping by binary logistic regression, analytical hierarchy process, and statistical index models and assessment of their performances. Nat Haz, 69, 749–779.

Pusgen. (2017): Earthquake Source and Disaster Map of Indonesia in 2017. Kementerian Pekerjaan Umum dan Perumahan rakyat, ISBN:978-602-5489-01-3. (*In Bahasa*)

Reichenbach, P., Busca, C., Mondini, A.C., and Rossi, M. (2014): The influence of land use change on landslide susceptibility zonation: the Briga catchment test site (Messina, Italy). Environ Manage., 54(6), 1372–1384. doi:10.1007/s00267-014-0357-0.

Resfiandhi, R., Sadisun, I.A., Sumaryono, and Triana, Y.D. (2014): A review on the features of earthquake induced landslides in Indonesia. In: International Conference of Transdisciplinary Research on Environmental Problems in Southeastern Asia (TREPSEA) 2014, Makassar, Indonesia, 4-5 September 2014.

Resfiandhi, R., Swana, G.W., Sadisun, I.A., and Sumaryono. (2015): Preliminary deterministic seismic landslide hazard maps of Tandikat area. In: Proceedings of 10th Asian Regional Conference of IAEG on "Geohazards and Engineering Geology", Kyoto, Japan, 26-29 September, 2015.

Sadisun, I. A., Telaumbanua, J. A., Kartiko, R. D., Dinara, I. A., and Pamela. (2021): Weight of Evidence Method for Landslide Susceptibility Mapping in Sigi Biromaru, Central Sulawesi. In: IOP Conference Series: Earth and Environmental Science, Volume 830, International Conference on Science, Infrastructure Technology and Regional Development 23-25 October 2020, South Lampung, Indonesia. doi: 10.1088/1755-1315/830/1/012029.

Saha, S., Saha, A., Hembram, T. K., Pradhan, B., and Alamri, A. M. (2020). Evaluating the Performance of Individual and Novel Ensemble of Machine Learning and Statistical Models for Landslide Susceptibility Assessment at Rudraprayag District of Garhwal Himalaya. Appl. Sci. 2020, 10(11), 3772; https://doi.org/10.3390/app10113772.

Saputra, A., Gomez, C., Hadmoko, D.S., and Sartohadi, J. (2016): Coseismic landslide susceptibility assessment using geographic information system. Geoenviron Disasters, 3, 27. https://doi.org/10.1186/s40677-016-0059-4.

Schlagel, N., Johnson, W.C., Deere, A.L., and Shroder, J.F. (2016): Multi-criteria analysis of landslide susceptibility,

Afghanistan. In: Geological Society of America Abstracts with Programs 48(7), GSA Annual Meeting, Denver, Colorado, USA, 25-28 September, 2016. doi: 10.1130/abs/2016AM-281520.

Sepúlveda, S.A., Murphy, W., and Petley, D.N. (2005): Topographic controls on coseismic rock slides during the 1999 Chi-Chi earthquake, Taiwan. Q J Eng Geol Hydrogeol, 38, 189–196.

Sidle, R.C., and Ochiai, H. (2006): Landslides: processes, prediction, and land use. American Geophysical Union.

Silalahi, F.E.S., Pamela, Arifianti, Y., Hidayat, F. (2019). Landslide susceptibility assessment using frequency ratio model in Bogor, West Java, Indonesia. Geosci. Lett. 6, 10. https://doi.org/10.1186/s40562-019-0140-4

Simandjuntak, T.O., Rusmana, E., Surono, and Supandjono, B.J. (1991): Geology of Malili Quadrangle, Sulawesi, scale 1:250.000. Geological Research and Development Centre, Bandung.

Sinčić, M., Bernat Gazibara, S., Krkač, M., and Mihalić Arbanas, S. (2022): Landslide susceptibility assessment of the City of Karlovac using the bivariate statistical analysis. Rudarsko-geološko-Naftni Zbornik, 37(2), 149–170. https://doi.org/10.17794/rgn.2022.2.13.

Socquet, A., Hollingsworth, J., Pathier, E., and Bouchon, M. (2019): Evidence of supershear during the 2018 magnitude 7.5 Palu earthquake from space geodesy. Nat Geosci, 12, 192-199. https://doi.org/10.1038/s41561-018-0296-0.

Sukamto, R. (1973): Reconnaissance geological map of Palu quadrangle, Sulawesi, scale 1:250.000. Geological Research and Development Centre Bandung.

Sukido, Sukarna, D., and Sutisna, K. (1993): Geological map of Pasangkayu quadrangle, Sulawesi, scale 1:250.000. Geological Research and Development Centre Bandung.

Sumaryono, Muslim, D., Sulaksana, N., and Triana, Y.D. (2015): Weights of evidence method for landslide susceptibility mapping in Tandikek and Damar Bancah, West Sumatra, Indonesia. IJSR, 4(10), 1283-1290.

Sumaryono, Triana, Y.D., Hidayati, S., Wahyudi, D.R., Muslim, D., and Sulaksana, N. (2015): Control Morphology to the Landslide Induced Earthquake: Case Study Padang Pariaman, Sumatra. In: Proceedings of 10th Asian Regional Conference of IAEG on "Geohazards and Engineering Geology", Kyoto, Japan, 26-29 September, 2015.

Sumaryono, Yohandi, K., Triana, Y.D., Iqbal, E.P., Santosa, I., Anjar, H., and Syatrin. (2018): Landslide and Debris Flow Risk. In: Andiani, Oktariadi O., Kurnia A. (eds) Di Balik Pesona Palu. Badan Geologi, 143-159. (*In Bahasa*)

Syifa, M., Kadavi, P.R., and Lee, C.W. (2019): An artificial intelligence application for post-earthquake damage mapping in Palu, Central Sulawesi, Indonesia. Sensors, 19(3), 542. doi: 10.3390/s19030542.

Tang, C., Zhu, J, Qi, X., and Ding, J. (2011): Landslides induced by the Wenchuan earthquake and the subsequent strong rainfall event: A case study in the Beichuan area of China. Eng Geol 122:22–33. doi.org/10.1016/j.enggeo.2011.03.013.

Tanoli, J. I., Ningsheng, C., Regmi, A. D., and Jun, L. (2017): Spatial distribution analysis and susceptibility mapping of landslides triggered before and after Mw7.8 Gorkha earthquake along Upper Bhote Koshi, Nepal. Arabian Journal of Geosciences 10-13.

Teerarungsigul, S., Torizin, J., Fuchs, M., Kühn, F., and Chonglakmani, C. (2015): An integrative approach for regional landslide susceptibility assessment using weight of evidence method: a case study of Yom River Basin, Phrae Province, Northern Thailand. Landslides, 13(5), 1151–1165. https://doi.org/10.1007/s10346-015-0659-1.

Tohari, A., Muttaqien, I., and Syifa, R. W. (2022): Understanding of flow liquefaction phenomena in Palu City from shear wave velocity profiles. In: Proceedings of The 13th of Aceh International Workshop and Expo on Sustainable Tsunami Disaster Recovery, https://doi.org/10.1051/e3s-conf/202234001011.

Torizin, J. (2011): Bivariate Statistical method for landslide susceptibility analysis using ArcGis. project of technical coperation 'Mitigation of Georisks'. BGR-Report publication. Hannover.

Umar, Z., Pradhan, B., Ahmad, A., Jebur, M.N., and Tehrany, M.S. (2014): Earthquake induced landslide susceptibility mapping using an integrated ensemble frequency ratio and logistic regression models in West Sumatera Province, Indonesia. Elsevier Science Direct Catena, 118, 124-135. https://doi.org/10.1016/j.catena.2014.02.005.

Ueno, T., and Shiiba, S. (2013): Landslides in Padang, West Sumatra, triggered by the September 2009 offshore earthquake. J Japan Landslide Soc, 6(1), 30-36. https://doi.org/10.13101/ijece.6.30.

United Nations General Assembly. (2016): Report of the Open-Ended Intergovernmental Expert 2 Working Group on Indicators and Terminology Relating to Disaster Risk Reduction. Seventy-First Session, Item 19(c). A/71/644.

USGS. (2018): M 7.5 - 70km N of Palu, Indonesia. https://earthquake.usgs.gov/earthquakes/eventpage/us1000h3p4/executive Accessed 23 June 2019.

van Leeuwen, T.M., and Muhardjo. (2005): Stratigraphy and tectonic setting of the Cretaceous and Paleogene volcanic-sedimentary successions in northwest Sulawesi, Indonesia: implications for the Cenozoic evolution of Western and Northern Sulawesi. J Asian Earth Sci, 25, 481-511 .

van Leeuwen, T.M., Allen, C.M., Elburg, M., Massone, H.J., Palin, J.M., and Hening, J. (2016): The Palu Metamorphic Complex, NW Sulawesi, Indonesia: Origin and evolution of a young metamorphic terrane with links to Gondwana and Sundaland. J Asian Earth Sci, 115, 133-152.

van Westen, C.J. (2000): The modelling of landslide hazards using GIS. Survey of Geo-physics, 21, 241-255.

van Westen, C.J, Castellanos, E., and Kuriakose, S.L. (2008): Spatial data for landslide susceptibility, hazard, and vulnerability assessment: An overview. Eng Geo, 102(3-4), 112-131. https://doi.org/10.1016/j.enggeo.2008.03.010.

Wang, F., Wafid, M.A.N., Zhang, F., and Takeuchi, A. (2011): Tandikek and Malalak rapid and long runout landslides triggered by West Sumatra earthquake 2009 (M7. 6) in Indonesia. Journal of the Japan Landslide Soc, 48(4), 215-220. https://doi.org/10.3313/jls.48.215.

Wang, X.Y., Nie, G.Z., and Wang, D.W. (2010): Relationships between ground motion parameters and landslides induced

by Wenchuan earthquake. Earthquake Science, 23(3), 233-242. doi:10.1007/s11589-010-0719-55.

Walpersdorf, A., and Vigny, C. (1998): Monitoring of the Palu-Koro Fault (Sulawesi) by GPS. Geophys Res Lett, 25(13), 2313–2316.

Watkinson, I.M. (2011): Ductile flow in the metamorphic rocks of central Sulawesi. In: Hall, R., Cottam, M.A., Wilson, M.E.J. (Eds), The SE Asian gateway: history and tectonics of Australia-Asia collision. Geo Soc London Spec Publ 355:445-453.

White, L.T., Hall, R., Armstrong, R.A., Barber, A.J., Fadel, M.B., Baxter, A., Wakita, K., Manning, C., and Soesilo, J. (2017): The geological history of the Latimojong region of western Sulawesi, Indonesia. J Asian Earth Sci, 138, 72-91.

Wubalem, A. (2021): Landslide susceptibility mapping using statistical methods in Uatzau catchment area, northwestern Ethiopia. Geoenviron Disasters 8, 1. https://doi.org/10.1186/s40677-020-00170-y.

Xu, Z., Che, A., Cao, Y., and Zhang, F. (2021): Seismic Landslide Susceptibility Assessment Using Principal Component Analysis And Support Vector Machine https://doi.org/10.21203/rs.3.rs-761260/v1.

Yang, Z.H., Lan, H. X., Gao, X., Li, L. P., Meng, Y. S., and Wu, Y. M. (2015): Urgent landslide susceptibility assessment in the 2013 Lushan earthquake-impacted area, Sichuan Province, China. Nat Hazard 75(3):2467–2487. doi.org/10.1007/s11069-014-1441-8.

Zhao,Y., Huang, Z., Wei, Z., Zheng, Z., and Konagai, K. (2023): Assessment of earthquake-triggered landslide susceptibility considering coseismic ground deformation. Front. Earth Sci. 10:993975. doi: 10.3389/feart.2022.993975.

Zhao, B. (2021): Landslides triggered by the 2018 Mw 7.5 Palu supershear earthquake in Indonesia. Elsevier Science Direct, Engineering Geology, 294, 106406. https://doi.org/10.1016/j.enggeo.2021.106406.

Zhou, S., Wang, W., Chen, G., Liu, B., and Fang, L. (2016): A Combined Weight of Evidence and Logistic Regression method for susceptibility mapping of earthquake-induced landslides: a case study of the April 20, 2013 Lushan earthquake. Acta Geologica Sinica, China.

Zieher, T., Perzl, F., Rössel, M., Rutzinger, M., Meßl, G., Markart, G., and Geitner, C. (2016): A multi-annual landslide inventory for the assessment of shallow landslide susceptibility – Two test cases in Vorarlberg, Austria. Geomorphology, 259, 40-54. https://doi.org/10.1016/j.geomorph.2016.02.008 .

SAŽETAK

Procjena podložnosti na klizišta inicirana potresom: potres od 7,5 Mw u 2018. godini u Paluu, Sulawesi, Indonezija

Katastrofalni potres koji se dogodio u Paluu 28. rujna 2018. godine, magnitude 7,5 Mw, izazvao je brojne nestabilnosti na padinama, uključujući nastanak velikoga broja klizišta. Ovaj rad predstavlja praktičnu metodu za definiranje procjene podložnosti na klizišta izazvana potresom u regiji Palu i okolnom području. Metoda *Weight of Evidence* (WoE) korištena je za procjenu odnosa između klizišta izazvanih seizmičkim kretanjem i preduvjeta kako bi se odredila razina podložnosti i izradila karta podložnosti na klizišta izazvana potresom u istraživanom području. 1273 klizišta podijeljena su u dvije serije podataka: podatci za treniranje modela (70 %) i podatci za validaciju modela (30 %). Korišteno je šest odabranih tematskih karata kao faktora koji utječu na pojavu klizišta: litologija, korištenje zemljišta, vršno ubrzanje tla (PGA), nagib padine, orijentacija padine i nadmorska visina. Odabir uzročnih faktora znatno utječe na učestalost klizišta na tom području. Rezultat modela zadovoljavajući je jer je vrijednost AUC odabranoga modela premašila minimalnu granicu koja iznosi 0,6 (60 %). Procijenjena uspješnost modela iznosi 85,7 %, što pokazuje relevantnost modela kod pojave klizišta. Stopa predviđanja od 84,6 % upućuje na to da je primijenjeni model vrlo dobar u predviđanju novih klizišta.

Ključne riječi:
potresom inicirana klizišta, karta podložnosti na klizišta, potres u Paluu, metoda *Weight of Evidence*

Author's contribution

Yukni Arifianti (Master, Associate Researcher, Landslide GIS Specialist) prepared the landslide data and the causative factors, wrote a major section of the paper, supervised the model and all the maps. **Pamela** (Master, First Mapping Surveyor, Landslide GIS Specialist) processed landslide data and the causative factors, AUC and WoE analysis. **Prahara Iqbal** (Dr, Associate Researcher, Engineering Geologist) provided the geology analysis and contributed in preparing the manuscript. **Sumaryono** (Dr, Associate Mapping Surveyor, Landslide Mitigation Specialist) contributed the landslide data and performed the field work. **Amalfi Omang** (Master, Associate Mapping Surveyor, Earthquake Mitigation Specialist) contributed the PGA analysis and performed the field work. **Hilda Lestiana** (Master, Associate Researcher, Remote Sensing Specialist) provided the remote sensing analysis and contributed in preparing the manuscript.